New Light-Harvesting Materials Using Accurate and Efficient Bandgap Calculations

Ivano E. Castelli, Falco Hüser, Mohnish Pandey, Hong Li, Kristian S. Thygesen, Brian Seger, Anubhav Jain, Kristin A. Persson, Gerbrand Ceder, and Karsten W. Jacobsen*

Electronic bandgap calculations are presented for 2400 experimentally known materials from the Materials Project database and the bandgaps, obtained with different types of functionals within density functional theory and (partial) self-consistent GW approximation, are compared for 20 randomly chosen compounds forming an unconventional set of ternary and quaternary materials. It is shown that the computationally cheap GLLB-SC potential gives results in good agreement (around 15%) with the more advanced and demanding eigenvalue-self-consistent GW. This allows for a high-throughput screening of materials for different applications where the bandgaps are used as descriptors for the efficiency of a photoelectrochemical device. Here, new light harvesting materials are proposed to be used in a one-photon photo-electrochemical device for water splitting by combining the estimation of the bandgaps with the stability analysis using Pourbaix diagrams and with the evaluation of the position of the band edges. Using this methodology, 25 candidate materials are obtained and 5 of them appear to have a realistic possibility of being used as photocatalyst in a one-photon water splitting device.

1. Introduction

High-throughput materials design is becoming more and more important in materials science thanks to theory developments that make computer simulations more reliable, and to an increase in computational resources. During the last decade,

Dr. I. E. Castelli, Dr. F. Hüser, M. Pandey, Dr. H. Li,
Prof. K. S. Thygesen, Prof. K. W. Jacobsen
Center for Atomic-scale Materials Design
Department of Physics
Technical University of Denmark
Kongens Lyngby, DK 2800, Denmark
E-mail: ivca@fysik.dtu.dk
Dr. B. Seger
Center for Individual Nanoparticle Functionality
Department of Physics
Technical University of Denmark
Kongens Lyngby, DK 2800, Denmark
Dr. A. Jain, Dr. K. A. Persson
Computational Research Division
Lawrence Berkeley National Laboratory
Berkeley, CA 94720, USA
Prof. G. Ceder
Massachusetts Institute of Technology
Cambridge, MA 02139, USA

the search for stable binary and ternary alloys,[1] batteries,[2] carbon capture and storage,[3] photovoltaics,[4,5] dye sensitized solar cells,[6] and water splitting materials[7,8] has been guided by computational studies. The huge amount of data produced during these studies has been collected in several databases, for example, the Materials Project database,[9] the AFLOWLIB consortium[1] and the Computational Materials Repository.[10,11]

Experimental data are also collected into databases such as the Inorganic Crystal Structure Database (ICSD)[12] and the Landolt-Börnstein database[13]: the former contains around 160 000 crystal structures, the latter collects the electronic, magnetic, thermodynamic properties of 250 000 compounds. The ICSD database is one of the most complete repositories for crystal information. Despite this, the electronic properties are not always available and so they are not included.

One of the tasks for computational condensed matter scientists is to fill in the missing information in experimental databases. In this paper, we present the calculations of around 2400 bandgaps of known materials using the GLLB-SC potential by Gritsenko, van Leeuwen, van Lenthe, and Baerends,[14] (GLLB) adapted by Kuisma et al.[15] to include the correlation for solids (-SC). The GLLB-SC potential is implemented in the framework of density functional theory (DFT) in the electronic structure code GPAW.[16,17] The structures under investigation are obtained from the Materials Project database.[9] As of March 2014, it contains around 50 000 structures optimized with DFT from the ICSD entries. We then compare the bandgaps of 20 compounds calculated with different methods, namely local density approximation (LDA), GLLB-SC, GW approximations (G_0W_0, GW_0, and GW) and the range-separated hybrid functional by Heyd, Scuseria, and Ernzerhof (HSE06). At the end, we apply a screening procedure, discussed in detail and used in previous works,[7,8] to find new light harvesting materials suitable for water splitting devices.

2. The Calculation of Bandgaps

Experimental databases mostly contain information about the crystal structure of materials. It is more complicated to

obtain access to information about the electronic structure of compounds. The bandgap is a key discriminating property for a large number of applications, including solar absorbers, thermoelectrics, transparent conductors, contact and buffer layers, etc. In recent works,[7,8] the bandgap has been used as a descriptor for the efficiency of a light absorber. In this part, we calculate the electronic bandgaps of experimentally known compounds. All the structures investigated here are available in the Materials Project database[9] and have been previously optimized using the generalized gradient approximation (GGA) functional by Perdew, Burke, and Ernzerhof (PBE), and GGA PBE+U for some of the structures.[18] While standard DFT usually gives good result for the optimization of the crystal structure, it fails in the calculation of bandgaps.[19] The Kohn-Sham bandgaps of semiconductors, given by the minimum energy difference between the bottom of the conduction band and the top of the valence band, are seriously underestimated because of the approximate description of the exchange-correlation functionals, the self-interaction error,[20] and the missing derivative discontinuity.[21] Many-body methods, such as the GW approximation, give more reliable results with an increase (at least one order of magnitude) of the computational cost. Hybrid functionals, e.g., PBE0 or HSE06, that incorporate a portion of Hartree-Fock exact exchange, usually give reasonable results for semiconductors,[22] but fail for metals and wide bandgap insulators.[23,24] All these methods are expensive to be used in a screening project of several thousands of materials and, in particular the GW approximation, can only be efficiently used to refine the results obtained with computationally cheaper approximations.[25]

Here, the bandgaps are calculated using the GLLB-SC functional,[16] that is an improved description of the original GLLB functional[14] adapted for solids. The GLLB functional contains by construction the evaluation of the derivative discontinuity. It is a further approximation to the KLI approximation to the exact exchange optimized effective potential (EXX-OEP).[26] The fundamental, or quasi-particle (QP), bandgap is given as the difference in the ionization potential (IP) and the electron affinity (EA) and thus directly linked to photo-emission and inverse photo-emission measurements. The Kohn-Sham (KS) bandgap differs from the QP gap by the derivative discontinuity, Δ_{xc}:

$$E_{gap}^{QP} = IP - EA = E_{gap}^{KS} + \Delta_{xc}. \tag{1}$$

GW, on the other hand, gives directly QP energies. It is important to keep in mind that the bandgaps obtained from optical measurements can be significantly lower than the QP gaps due to excitonic effects, and one thus speaks of an optical bandgap instead.[27]

The GLLB-SC functional has been recently tested against other computational methods (mainly non-self-consistent G_0W_0) and experiments for single metal oxides,[8] for semiconductors,[28] and for perovskite materials for light harvesting.[25] The GLLB-SC results are expected to be within an error of 0.5 eV. We thus expect that this accuracy is good enough for projects involving thousands of calculations required in a screening study. In addition, with the GLLB-SC is possible to calculate larger crystal structures. For example, recently, the GLLB-SC has been widely used to calculate the bandgaps of 240 organometal halide perovskites[29] which show very interesting optical properties for light harvesting and energy conversion.[30] We note that the GLLB-SC has also given good results for the position of the d-states in noble metals such as silver.[31]

The Materials Project database is constantly updated and so far we have calculated the bandgaps of around 2400 materials. Those materials have been selected because of their relative simple structure, their stability and because they show a bandgap at the GGA level. Despite its low computational cost, the GLLB-SC functional is at least twice as expensive as a standard GGA calculation[32] and it is demanding to calculate the bandgaps of large crystal structures of more than 40/50 atoms. Around 6 months has been the computational time required for the bandgap calculations for the 2400 materials using Niflheim, the supercomputer facility installed at DTU Physics. On a single core machine, the time required would have been around 16.5 years. All the calculated quasi-particle gaps, together with the corresponding ids from the Materials Project and ICSD databases and the chemical formula, are listed in the Supporting Information. In addition, this information is included and freely available in both the Materials Project database and the Computational Materials Repository.

The distribution of the bandgaps, calculated with GLLB-SC, of the 2400 materials is shown in **Figure 1** (in blue). Even though very large bandgap insulators have been found, the region with a large number of materials correspond to the visible light range, between 1.5 and 3.0 eV. When the stability in water at pH = 7 and at potential 0 V versus normal hydrogen electrode (NHE) is considered by means of Pourbaix diagrams,[33] the number of materials that might be stable is significantly reduced. The Pourbaix diagrams give information about the thermodynamics of the reactions, while other factors, such as kinetics and surfaces passivation, are not included. For these and other reasons, here we have considered two energy thresholds to define if a material is stable ($\Delta E = 1$ and 0 eV/atom, shown in red and green bars in the figure, where ΔE is the total energy difference between the material and the most stable phases in which it can separate). Within the energy threshold of 1 eV/atom, more than 50% of the small bandgap semiconductors are unstable in water, while it seems that all the materials
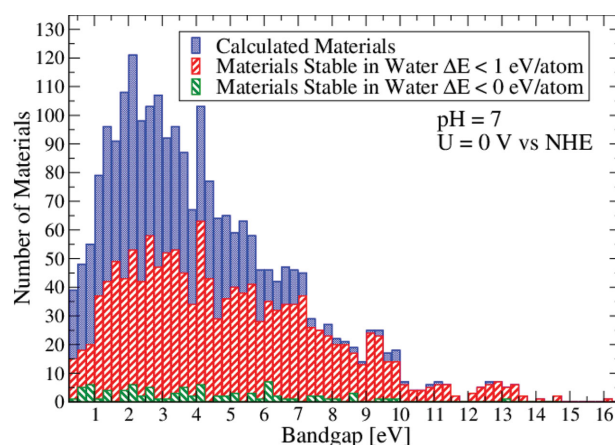
Figure 1. Histogram of the GLLB-SC bandgaps for all the 2400 calculated materials (in blue). We consider the two energy thresholds 1 eV/atom (in red) and 0 eV/atom (in green) for the stability in water, which is calculated at zero potential ($U = 0$ V vs NHE) and neutral pH.
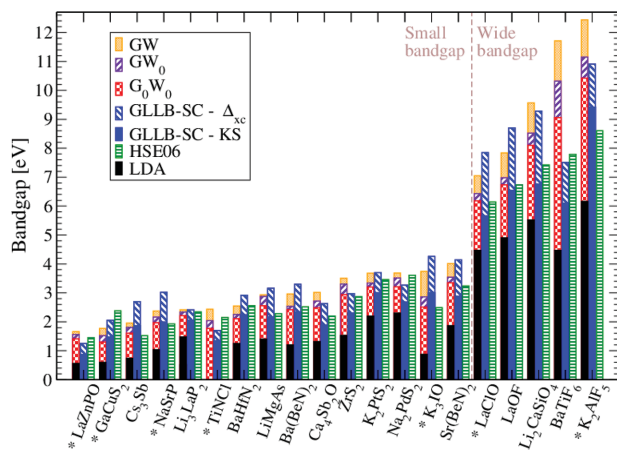
Figure 2. Bandgaps at Γ-point of 20 structure calculated with LDA (in black), GW approximations with PPA (G_0W_0 in red, GW_0 in purple and GW in orange), GLLB-SC (in blue), and HSE06 (in green). Both the KS bandgap and the derivative discontinuity are indicated for the GLLB-SC gaps. The materials for which the Γ-point gap corresponds to the bandgap, are indicated with *.

with a gap larger that 10 eV are stable in water. Only around 4% of the materials are stable, when the more strict threshold of 0 eV/atom is used. This may indicate that considering a ΔE larger than zero can help to identify the materials that are experimentally observed to be stable in water.

The electronic structures of 20 materials, randomly picked from the calculated set to cover the full bandgap range and with a reasonable unit cell size, were also calculated using the non-self-consistent G_0W_0 and the eigenvalue-self-consistent GW_0 and GW as well as the HSE06 hybrid scheme (**Figure 2**). This unconventional set of structures contains ternary and quaternary materials including oxides, nitrides, sulfides, phosphates and chlorides and thus it is a broader set compared to the ones used elsewhere in the literature.[34]

QP gaps were obtained in the G_0W_0 approximation in a plane wave representation using LDA wavefunctions and eigenvalues as starting point. A detailed description of the implementation of this method in GPAW can be found in ref. [28]. The initial Kohn-Sham states and energies were calculated in a plane wave basis with kinetic energies up to 600 eV. The same value is used for determining the exact exchange contributions. The G_0W_0 self-energy was carefully converged with respect to k points, number of bands and plane wave cutoff energy for each material individually. Typically, a $(7 \times 7 \times 7)$ k-point sampling, 100–200 eV energy cutoff and unoccupied bands up to the same energy (a few hundred bands in total) were found to be sufficient in order to converge band gaps within less than 0.1 eV. Both, the plasmon pole approximation (PPA) by Godby and Needs[35] and the explicit frequency dependence of the dielectric function, $\varepsilon(\omega)$, have been used, yielding almost identical results.

It is well known that G_0W_0 underestimates bandgaps compared to experiments and better results can be obtained using (partial) self-consistent GW[34] where the LDA wavefunctions are kept fixed while the eigenvalues are updated self-consistently. Recently,[28] it was shown for a set of well known semiconductors and insulators, that the MAEs for GLLB-SC and

G_0W_0 with respect to experiments are 0.4 and 0.3 eV, respectively, with a tendency of the former to overestimate the gaps, while the latter underestimates them.

Two levels of (partial) self-consistency have been investigated: i) in the case of GW_0, the self-consistency in the eigenvalues is performed for the Green's functions (G) only, whereas ii) in the case of GW, the eigenvalues are updated both in G and in the dielectric matrix of the screened potential (W). In general, for the 20 materials described in this section, three or four iterations are necessary to converge band gaps within less than 30 meV and 50 meV for GW_0 and GW, respectively. Due to the high computational costs, the k-point mesh and energy cutoff used for GW_0 and GW are coarser than the ones used for G_0W_0. Typically the low convergence criteria of $(3 \times 3 \times 3)$ k-point sampling and 100 eV energy cutoff are used for GW_0 and GW. The band gaps are then extrapolated to the dense k-point grids and high plane wave cut off, using the difference between the low and high convergence parameters in the G_0W_0 calculations. For more details about GW_0 and GW, see ref. [34] and references therein.

Hybrid functional based calculations were performed with the range-separated screened-exchange HSE06 functional.[36,37] The wavefunctions were expanded in a plane-wave basis with a 700 eV cutoff. We use a Monkhorst-Pack[38] grid of $33 \times (a_x^{-1}, a_y^{-1}, a_z^{-1})$ k-points, where a_x, a_y and a_z are the lattice constants in x, y and z direction, respectively, and the Γ-point is always included. In the current work, all HSE06 calculations were performed non-self-consistently from the PBE ground state density and wavefunctions. Generally, there is good agreement between the non-self-consistent calculations and the self-consistently obtained results[24] which indicates that self-consistency will not be important in the current work.

For all materials in this study, comparison between the different methods is shown by means of the direct Γ point gap, in order to avoid the need for interpolation of the band structure in the case that the minimum of the conduction band is not located at a high symmetry point in the Brillouin zone.

Figure 2 shows the bandgaps for the 20 selected materials calculated with LDA, different levels of the GW approximation, HSE06, and GLLB-SC. Only a few experimental data points are available, and mainly optical measurements which are therefore not directly comparable with our values. Ideally photoemission and inverse photoemission measurements could be used to compare to our calculated bandgaps, but these are not available for this set of structures.

It is natural to divide the 20 materials into small and wide bandgap semiconductors to give a better evaluation of the signed and mean absolute and relative errors[39] for the different methods studied here (**Table 1** for the small gap set). Similar data for the wide gaps is reported in the Supporting Information together with the comparison of band structures calculated with different methods for two compounds.

As expected, for both the groups, LDA seriously underestimates the bandgaps. The mean absolute error (MAE) of GLLB-SC with respect to G_0W_0 and to HSE06 is larger than 0.5 eV for the small bandgaps with a clear tendency for GLLB-SC to overestimate the bandgaps with respect to HSE06 and to G_0W_0 as shown by the signed error and **Figure 3**a,b. G_0W_0 and HSE06 are very close, with a MAE of approximately 0.25 eV (G_0W_0

Table 1. Mean absolute (signed) error, in eV, for the small bandgaps of the materials in Figure 2 calculated using LDA, GLLB-SC, HSE06, G_0W_0, GW_0 and GW.

xc_{ref}	LDA	GLLB-SC	HSE06	G_0W_0	GW_0	GW
xc						
LDA	–	1.64 (−1.64)	1.21 (−1.21)	1.08 (−1.08)	1.30 (−1.30)	1.59 (−1.59)
GLLB-SC	1.64 (1.64)	–	0.61 (0.43)	0.59 (0.56)	0.52 (0.34)	0.38 (0.05)
HSE06	1.21 (1.21)	0.61 (−0.43)	–	0.25 (0.13)	0.29 (−0.09)	0.46 (−0.38)
G_0W_0	1.08 (1.08)	0.59 (−0.56)	0.25 (−0.13)	–	0.22 (−0.22)	0.51 (−0.51)
GW_0	1.30 (1.30)	0.52 (−0.34)	0.29 (0.09)	0.22 (0.22)	–	0.29 (−0.29)
GW	1.59 (1.59)	0.38 (−0.05)	0.46 (0.38)	0.51 (0.51)	0.29 (0.29)	–

underestimates with respect to HSE06). The GW_0 approximation gives a MAE of around 0.5 eV for the GLLB-SC and slightly less than 0.3 eV for HSE06 and the other two GW levels. The GLLB-SC is the closest to the self-consistent GW with a MAE of 0.38 eV when compared with HSE06 and G_0W_0 which have a MAE close to 0.5 eV.

GLLB-SC has a mean relative errors (MRE) with respect to GW equal to 15% better that the MRE for HSE06 and G_0W_0 (16 and 18%, respectively), while GW_0 performs better with an error of 10%. The HSE06 error increases to 23% for the wide bandgap set, as shown in the Supporting Information.

The computational costs required for the methods are very different. G_0W_0 is one or two orders of magnitude more expensive that GLLB-SC which is slightly more expensive than a standard GGA calculation. HSE06 is slightly more expensive than GLLB-SC but still cheaper than G_0W_0. The computational cost increases even further for the (partial) self-consistent GW where more iterations are needed.

Figure 3. a) HSE06, b) G_0W_0, c) GW_0, and d) GW bandgaps as a function of the GLLB-SC gaps. All the methods except GW underestimate the gaps with respect to the GLLB-SC. The signed error of GLLB-SC and GW is 0.05 eV.

The bandgaps calculated with GLLB-SC can now be used as a descriptor in a screening study. In the following section, we propose a handful of materials that can be used in a water splitting device using a high-throughput screening approach.

3. Screening for Water Splitting Materials

The starting point of a screening study is to define the descriptors that correlate the microscopic quantities calculated using ab-initio quantum mechanics simulations with the macroscopic properties of a material.[40] For example, the formation enthalpy of a compound can describe its stability, the bandgap its absorption properties, and so on.

The set of data calculated here can provide the search space for the computational screening of materials for different applications, such as light absorbers (photovoltaics and photocatalysis), transparent conductors, and thermoelectrics. Here, we illustrate this approach by proposing a handful of materials that can be used to produce energy through photoelectrochemical splitting of water into oxygen and hydrogen using solar light. In a water splitting device, solar energy is used to divide water into hydrogen and oxygen: the solar light is harvested by a semiconductor and electron-hole pairs are created. The electrons and holes then reach the surface of the semiconductor where, if they are at the right potentials with respect to the redox levels of water, the electrons reduce the protons and the holes oxidize the water. The properties required by a semiconductor to be used in this device are: i) stability, ii) high light absorption, iii) photogenerated charges with appropriate energies. In addition iv) good electron-hole mobility, v) high catalytic activity, vi) non-toxicity, and vii) cost-effectiveness are desirable properties. The screening is based on three criteria: stability, bandgap in the visible light range, and band edges of the semiconductor well positioned versus the redox levels of water. These represent the descriptors for the properties (i–iii), i.e., a stable material with a well positioned bandgap in the visible light range. A more detailed explanation of the water splitting device can be found in previous works.[7,8]

Previous studies have described the search for new compounds to be used in a water splitting cell both in the perovskite crystal symmetry (cubic,[7,8] double,[41] and layered in the Ruddlesden Popper phase[25]) and in the oxynitride and nitride class of materials using a data mining approach.[42] Here, instead of searching for completely new materials, we consider structures
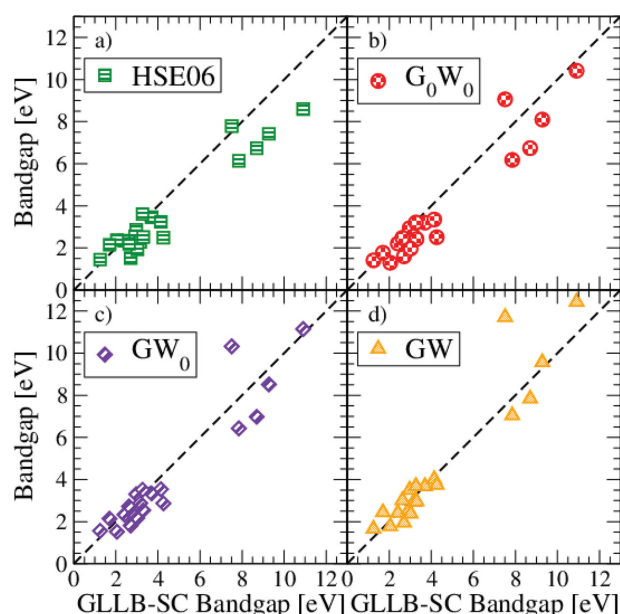
already optimized by nature, i.e., known to exist. While no new compounds will be proposed, this scheme has the advantage of the known synthesis procedure so that testing and validation can be prioritized.

Although all the materials studied here are experimentally known, i.e., they are stable, or at least metastable, little is known about their stability in contact with water. The corrosion problem can be investigated using the so-called Pourbaix diagrams, where solid and dissolved substances are combined in a single phase diagram so that the stable species (solid and/or aqueous ion) can be determined, as a function of pH and potential. The total energies of the solid phases, taken from the ICSD and the Materials Project databases,[9,12] are obtained with DFT (using the RPBE xc-functional[43]). Data for the dissolved ions, instead, come from experiments.[44,45] This method for evaluating stability in water has been already investigated and validated elsewhere.[33,46]

It is difficult to define a single energy threshold under which a material is considered stable because of metastability, reaction kinetics, effect and passivation of the surfaces as well as inaccuracy in the calculations and experiments. Here, we consider a generous energy threshold of 1 eV/atom. We propose 25 compounds (**Figure 4**), that also fulfill the criteria relating to the bandgap and band edges positions, stable in a potential window corresponding to the working potential of the device (bare redox levels of water plus reaction overpotentials and quasi-Fermi levels, i.e., between −0.4 and 2.2 V) and in neutral pH (pH = 7). Neutral pH is desirable because it is not harmful to environment and not corrosive however the efficiency of the device can be improved by operating at very acid or alkaline conditions.

The bandgaps have been calculated with the GLLB-SC functional. The bare energy required to split water is 1.23 eV. This energy is not enough to run the water splitting reactions and some overpotentials are needed (0.1 eV for hydrogen evolution and 0.4 eV for oxygen production[47]). When the semiconductor is under illumination and electron-hole pairs are created, the electron and hole densities are above their equilibrium values and a single Fermi level cannot describe their populations. The quasi-Fermi levels describe these non-equilibrium populations, located ≈0.25 eV below (above) the conduction (valence) bands for an undoped semiconductor and they correspond to the effective energy of the photogenerated electrons and holes. The minimum bandgap to run the water splitting reaction is at least 2 eV. The maximum realistic efficiency of a water splitting device is around 7%.[48] This efficiency is quite low, especially when compared with the standard technologies for photovoltaics. A higher efficiency can be obtained using a multiphoton device[7,49] albeit increasing the technological difficulties and thus the price of the device. In this work, we focus on the one-photon device emphasizing the simplicity of the device rather than efficiency.[50]

There are several methods to obtain the positions of the band edges,[51,52] all computationally rather demanding and not suited to be used in a screening study. Here, the positions of the band edges have been calculated using an empirical equation based on the geometrical average of the electronegativities in the Mulliken scale of the individual atoms that form the
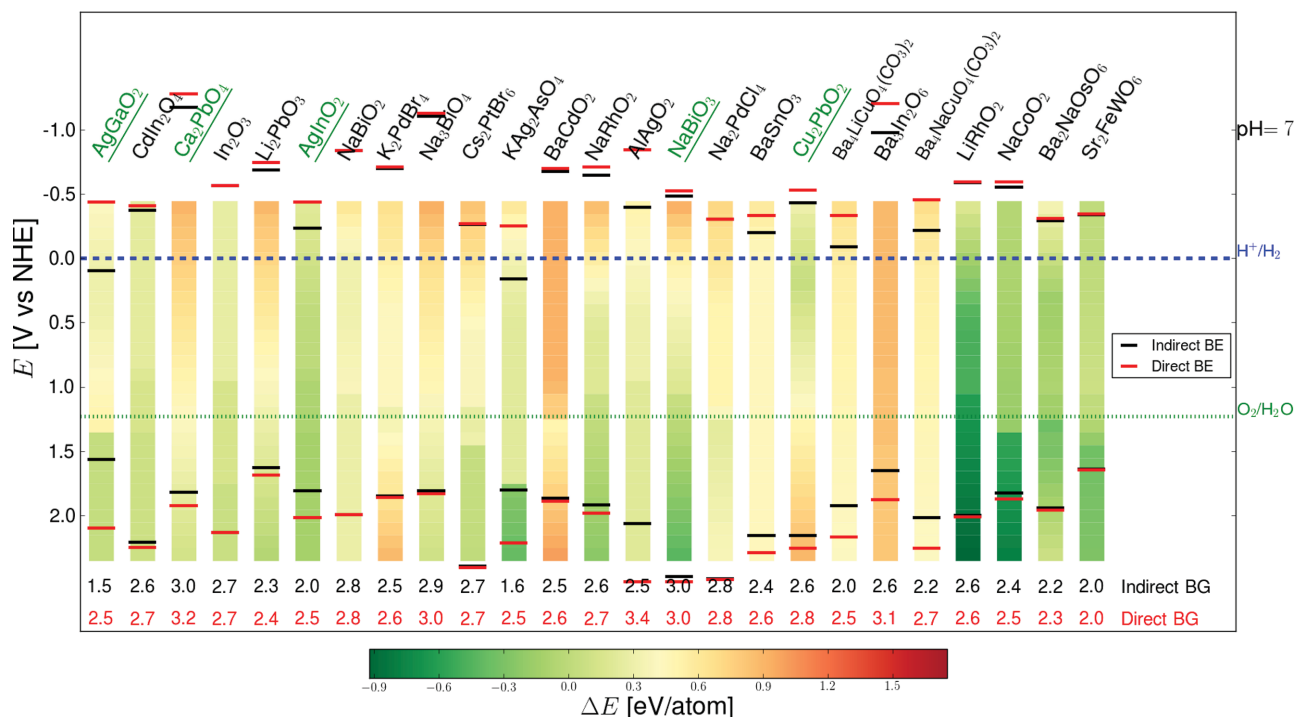
Figure 4. The most stable materials with potential for one-photon water splitting. The stability in water of each material is calculated as the energy difference between the material and the most stable phases (solid and aqueous) in which it can separate in a potential range between −0.4 and 2.2 V and at pH = 7. The color scale runs from green (i.e., stable) to red (unstable compounds). In the plot, the indirect and direct positions of the valence and conduction band edges (BE) are indicated in black and red as well as the indirect and direct bandgap (BG).

FULL PAPER

structure.[53] For example, the valence (conduction) band edges of ZrS_2 is:

$$E_{VB,CB} = (\chi_{Zr} \chi_S^2) \pm E_{gap}/2 + E_0, \qquad (2)$$

where χ_{Zr} and χ_S are the electronegativities of Zr and S, E_{gap} the calculated bandgap, and $E_0 = -4.5$ V the difference between the normal hydrogen electrode (NHE) and vacuum level.

The screening criteria can be summarized as: stability in water: $\Delta E \leq 1.0$ eV/atom; bandgap: $1.7 \leq E_{gap} \leq 3.0$ eV; and band edges position: $CB_{edge} < -0.1$ V vs NHE and $VB_{edge} > 1.6$ V vs NHE.

Figure 4 shows the 25 stable semiconductors fulfilling the screening requirements out of the 2400 calculated materials. The figure combines the evaluation of the stability using Pourbaix diagrams, calculated at pH = 7 and in a potential range between −0.4 and 2.2 eV, where stable and unstable compounds are indicated in green and red, and the indirect and direct positions of the valence and conduction band edges are drawn with black and red lines, respectively. In particular, oxides tend to be more stable at the oxidative potential, as the O_{2p} orbitals, that usually form the valence band of oxides, are low in energy and thermodynamically favorable. In general, the problem of stability in water is important but not crucial to the design a new light harvester material. Necessarily, the photoharvester can be protected by transparent protective shields that remove the problem of corrosion due to water and oxygen and hydrogen ions in solution.[54] On the other hand, the use of a transparent shield increases the manufacturing difficulties and the total cost of the photodevice.

We performed a literature search for available information of the candidate materials of Figure 4. In particular, we are interested in data regarding stability in water, light absorption, and industrial applications. Five materials of Figure 4 (green underlined formula) have a realistic possibility of success as a one-photon photocatalytic water splitting material. Ca_2PbO_4 has an optical bandgap of approximately 1.8 eV[55] and it is used as a primer for stainless steel due to its lower toxicity compared to lead oxide.[56] Cu_2PbO_2 was originally synthesized by Szillat et al. and they showed the material was insoluble in basic solutions.[57] This compound has an optical bandgap of 1.7 eV and is naturally p-type semiconductor.[58] α-AgGaO$_2$ has been shown to have a bandgap of 2.4 eV whereas a bandgap of 2.1–2.2 eV has been found for β-AgGaO$_2$.[59,60] $AgInO_2$ has a bandgap of 1.9 eV.[60] $AgGaO_2$ and $AgInO_2$ have been successfully tested for photocatalytic degradation of alcohols.[59,60] $NaBiO_3$ has a bandgap of 2.6 eV, and has already been used for photocatalytic degradation of pollutants.[61] Using computational modeling, Liu et al. found a bandgap of 2.2 eV and a valence and conduction band that straddles the water splitting redox reactions.[62]

Some materials show an experimental bandgap above 3.0 eV and thus are unsuited for an effective water splitting catalyst. For example, $BaSnO_3$, which has already been proposed as a light harvester material in previous work[7,8] in which the cubic perovskites have been investigated, has a bandgap of 3.1–3.3 eV and luminesces at 1.4 eV.[63] It has been tested for photochemical H_2 and O_2 evolution using sacrificial donors, however its water splitting activity is inhibited due to defect-assisted recombination.[64] In_2O_3 has a bandgap near 3.4 eV (however some papers report a bandgap of 2.8 eV[65]) and a conduction band near 0.00 V vs RHE.[66] It has been used as a photocatalyst[67] or to enhance the catalytic performances of photocatalysts, such as $LaTiO_2N$.[68] A detailed analysis of all the candidate materials is reported in the Supporting Information.

4. Conclusions

In this work, we have calculated the bandgaps of approximately 2400 known materials, available in the Materials Project database, using a recently implemented functional that includes the evaluation of the derivative discontinuity.

As a first step, we compared the bandgaps calculated with the GLLB-SC potential with several levels of the GW approximation and hybrid HSE06 scheme for 20 materials. We showed that the agreement between GLLB-SC and GW is rather good, with a MRE of around 15% better than the agreement between G_0W_0 (or HSE06) and GW and with a significant savings in the computational cost.

Secondly, we have applied a screening procedure to the set of calculated materials with the goal of finding new materials to be used in a one-photon water splitting device. We combined the calculation of the bandgaps with the evaluation of Pourbaix diagrams to estimate the materials' stability in water with the evaluation of the band edge positions to determine whether the photogenerated charges carry the energy necessary to initiate a water splitting reaction. An a posteriori literature search shows that at least five of them (Ca_2PbO_4, Cu_2PbO_2, $AgGaO_2$, $AgInO_2$, and $NaBiO_3$) might be suitable to be used in a water splitting device and require further experimental investigation.

The calculated data may be of relevance for other applications within sustainable energy materials and all the data are made available to the public in the Materials Project database and in the Computational Materials Repository.

Supporting Information

Supporting Information is available from the Wiley Online Library or from the author.

Acknowledgments

[1] S. Curtarolo, W. Setyawan, G. L. Hart, M. Jahnatek, R. V. Chepulskii, R. H. Taylor, S. Wang, J. Xue, K. Yang, O. Levy, M. J. Mehl, H. T. Stokes, D. O. Demchenko, D. Morgan, *Comput. Mater. Sci.* **2012**, *58*, 218.

[2] G. Ceder, Y.-M. Chiang, D. R. Sadoway, M. K. Aydinol, Y.-I. Jang, B. Huang, *Nature* **1998**, *392*, 694.

[3] L.-C. Lin, A. H. Berger, R. L. Martin, J. Kim, J. A. Swisher, K. Jariwala, C. H. Rycroft, A. S. Bhown, M. W. Deem, M. Haranczyk, B. Smit, *Nat. Mater.* **2012**, *11*, 633.

[4] J. Hachmann, R. Olivares-Amaya, S. Atahan-Evrenk, C. Amador-Bedolla, R. S. Sanchez-Carrera, A. Gold-Parker, L. Vogt, A. M. Brockway, A. Aspuru-Guzik, *J. Phys. Chem. Lett.* **2011**, *2*, 2241.

[5] M. d'Avezac, J.-W. Luo, T. Chanier, A. Zunger, *Phys. Rev. Lett.* **2012**, *108*, 027401.

[6] K. B. Ørnsø, J. M. Garcia-Lastra, K. S. Thygesen, *Phys. Chem. Chem. Phys.* **2013**, *15*, 19478.

[7] I. E. Castelli, D. D. Landis, K. S. Thygesen, S. Dahl, I. Chorkendorff, T. F. Jaramillo, K. W. Jacobsen, *Energy Environ. Sci.* **2012**, *5*, 9034.

[8] I. E. Castelli, T. Olsen, S. Datta, D. D. Landis, S. Dahl, K. S. Thygesen, K. W. Jacobsen, *Energy Environ. Sci.* **2012**, *5*, 5814.

[9] Materials Project - A Materials Genome Approach, http://materialsproject.org/ (accessed August 2014) .

[10] D. D. Landis, J. S. Hummelshoj, S. Nestorov, J. Greeley, M. Dulak, T. Bligaard, J. K. Norskov, K. W. Jacobsen, *J. Comput. Sci. Eng.* **2012**, *14*, 51.

[11] Computational Materials Repository, https://cmr.fysik.dtu.dk/ (accessed August 2014).

[12] ICSDWeb, http://www.fiz-karlsruhe.de/icsd_web.html (accessed July 2014).

[13] The Landolt-Börnstein Database, http://www.springermaterials.com/docs/index.html (accessed May 2014).

[14] O. Gritsenko, R. van Leeuwen, E. van Lenthe, E. J. Baerends, *Phys. Rev. A* **1995**, *51*, 1944.

[15] M. Kuisma, J. Ojanen, J. Enkovaara, T. T. Rantala, *Phys. Rev. B* **2010**, *82*, 115106.

[16] J. J. Mortensen, L. B. Hansen, K. W. Jacobsen, *Phys. Rev. B* **2005**, *71*, 35109.

[17] J. Enkovaara, C. Rostgaard, J. J. Mortensen, J. Chen, M. Dulak, L. Ferrighi, J. Gavnholt, C. Glinsvad, V. Haikola, H. A. Hansen, H. H. Kristoffersen, M. Kuisma, A. H. Larsen, L. Lehtovaara, M. Ljungberg, O. Lopez-Acevedo, P. G. Moses, J. Ojanen, T. Olsen, V. Petzold, N. A. Romero, J. Stausholm-Møller, M. Strange, G. A. Tritsaris, M. Vanin, M. Walter, B. Hammer, H. Häkkinen, G. K. H. Madsen, R. M. Nieminen, J. K. Nørskov, M. Puska, T. T. Rantala, J. Schiøtz, K. S. Thygesen, K. W. Jacobsen, *J. Phys. Condens. Matter* **2010**, *22*, 253202.

[18] A. Jain, S. P. Ong, G. Hautier, W. Chen, W. D. Richards, S. Dacek, S. Cholia, D. Gunter, D. Skinner, G. Ceder, K. A. Persson, *APL Mater.* **2013**, *1*, 011002.

[19] J. P. Perdew, *Int. J. Quantum Chem.* **1985**, *28*, 497.

[20] J. P. Perdew, A. Zunger, *Phys. Rev. B* **1981**, *23*, 5048.

[21] R. W. Godby, M. Schlüter, L. J. Sham, *Phys. Rev. Lett.* **1986**, *56*, 2415.

[22] J. Heyd, J. E. Peralta, G. E. Scuseria, R. L. Martin, *J. Chem. Phys.* **2005**, *123*, 174101.

[23] J. E. Moussa, P. A. Schultz, J. R. Chelikowsky, *J. Chem. Phys.* **2012**, *136*, 204117.

[24] J. Paier, M. Marsman, K. Hummer, G. Kresse, I. C. Gerber, J. G. Ángyán, *J. Chem. Phys.* **2006**, *124*, 154709.

[25] I. E. Castelli, J. M. García-Lastra, F. Hüser, K. S. Thygesen, K. W. Jacobsen, *New J. Phys.* **2013**, *15*, 105026.

[26] J. D. Talman, W. F. Shadwick, *Phys. Rev. A* **1976**, *14*, 36.

[27] G. Onida, L. Reining, A. Rubio, *Rev. Mod. Phys.* **2002**, *74*, 601.

[28] F. Hüser, T. Olsen, K. S. Thygesen, *Phys. Rev. B* **2013**, *87*, 235132.

[29] I. E. Castelli, J. M. García-Lastra, K. S. Thygesen, K. W. Jacobsen, *APL Mater.* DOI: 10.1063/1.4893495.

[30] I. Borriello, G. Cantele, D. Ninno, *Phys. Rev. B* **2008**, *77*, 235214.

[31] J. Yan, K. W. Jacobsen, K. S. Thygesen, *Phys. Rev. B* **2011**, *84*, 235430.

[32] Typically a k-point mesh finer than a GGA calculation is required. For the calculations presented here, we have used a k-point sampling equal to $35 \times a_i^{-1}$ in each direction, where a_i is the lattice constant, with Γ-point are included.

[33] I. E. Castelli, K. S. Thygesen, K. W. Jacobsen, *Top. Catal.* **2013**, *57*, 1.

[34] M. Shishkin, G. Kresse, *Phys. Rev. B* **2007**, *75*, 235102.

[35] R. W. Godby, R. J. Needs, *Phys. Rev. Lett.* **1989**, *62*, 1169.

[36] J. Heyd, G. E. Scuseria, M. Ernzerhof, *J. Chem. Phys.* **2003**, *118*, 8207.

[37] A. V. Krukau, O. A. Vydrov, A. F. Izmaylov, G. E. Scuseria, *J. Chem. Phys.* **2006**, *125*, 224106.

[38] H. J. Monkhorst, J. D. Pack, *Phys. Rev. B* **1976**, *13*, 5188.

[39] The signed error (SE), is calculated as $\text{SE} = \frac{1}{n}\sum_n E_{gap}^{xc} - E_{gap}^{xc_{ref}}$, and the mean absolute error (MAE) as $\text{MAE} = \frac{1}{n}\sum_n \left| E_{gap}^{xc} - E_{gap}^{xc_{ref}} \right|$, where E_{gap}^{xc} indicates the bandgaps calculated with the test exchange-correlation (xc) functional, $E_{gap}^{xc_{ref}}$ and the bandgaps obtained with the reference functional. The mean relative error (MRE) is given by $\text{MRE} = \frac{1}{n}\sum_n \left| \frac{E_{gap}^{xc} - E_{gap}^{xc_{ref}}}{E_{gap}^{xc_{ref}}} \right|$.

[40] S. Curtarolo, G. L. W. Hart, M. B. Nardelli, N. Mingo, S. Sanvito, O. Levy, *Nat. Mater.* **2013**, *12*, 191.

[41] I. E. Castelli, K. S. Thygesen, K. W. Jacobsen, *MRS Online Proc. Lib.* **2013**, *1523*.

[42] Y. Wu, P. Lazic, G. Hautier, K. Persson, G. Ceder, *Energy Environ. Sci.* **2013**, *6*, 157.

[43] B. Hammer, L. B. Hansen, J. K. Nørskov, *Phys. Rev. B* **1999**, *59*, 7413.

[44] J. W. Johnson, E. H. Oelkers, H. C. Helgeson, *Computers Geosci.* **1992**, *18*, 899.

[45] M. Pourbaix, *Atlas of Electrochemical Equilibria in Aqueous Solutions*, v. 1, Pergamon Press, London **1966**.

[46] K. A. Persson, B. Waldwick, P. Lazic, G. Ceder, *Phys. Rev. B* **2012**, *85*, 235438.

[47] S. Trasatti, *Croat. Chem. Acta*, **1990**, *63*, 313.

[48] M. R. Weber, M. J. Dignam, *Int. J. Hydrogen Energy* **1986**, *11*, 225.

[49] M. Gratzel, *Nature* **2001**, *414*, 338.

[50] B. A. Pinaud, J. D. Benck, L. C. Seitz, A. J. Forman, Z. Chen, T. G. Deutsch, B. D. James, K. N. Baum, G. N. Baum, S. Ardo, H. Wang, E. Millere, T. F. Jaramillo, *Energy Environ. Sci.* **2013**, *6*, 1983.

[51] Y. Wu, M. K. Y. Chan, G. Ceder, *Phys. Rev. B* **2011**, *83*, 235301.

[52] P. G. Moses, C. G. V. de Walle, *Appl. Phys. Lett.* **2010**, *96*, 021908.

[53] M. A. Butler, D. S. Ginley, *J. Electrochem. Soc.* **1978**, *125*, 228.

[54] B. Seger, A. B. Laursen, P. C. K. Vesborg, T. Pedersen, O. Hansen, S. Dahl, I. Chorkendorff, *Angew. Chem. Int. Ed.* **2012**, *51*, 9128.

[55] R. P. Diez, E. J. Baran, A. E. Lavat, M. C. Grasselli, *J. Phys. Chem. Solids* **1995**, *56*, 135.

[56] K. Rubesova, D. Sykorova, *J. Sol-Gel Sci. Technol.* **2009**, *49*, 228.

[57] H. Szillat, C. L. Teske, *Z. Anorg. Allge. Chem.* **1994**, *620*, 1307.

[58] H. Yanagi, J. Tate, R. Nagarajan, A. W. Sleight, *Solid State Commun.* **2002**, *122*, 295.

[59] Y. Maruyama, H. Irie, K. Hashimoto, *J. Phys. Chem. B* **2006**, *110*, 23274.

[60] S. X. Ouyang, N. Kikugawa, D. Chen, Z. G. Zou, J. H. Ye, *J. Phys. Chem. C* **2009**, *113*, 1560.

[61] T. Kako, Z. G. Zou, M. Katagiri, J. H. Ye, *Chem. Mater.* **2007**, *19*, 198.

[62] J. J. Liu, S. F. Chen, Q. Z. Liu, Y. F. Zhu, J. F. Zhang, *Chem. Phys. Lett.* **2013**, *572*, 101.

[63] H. Mizoguchi, P. M. Woodward, C. H. Park, D. A. Keszler, *J. Am. Chem. Soc.* **2004**, *126*, 9796.

[64] W. Zhang, J. Tang, J. Ye, *J. Mater. Res.* **2007**, *22*, 1859.

[65] J. Lv, T. Kako, Z. Li, Z. Zou, J. Ye, *J. Phys. Chem. C* **2010**, *114*, 6157.

[66] E. Y. Wang, L. Hsu, *J. Electrochem. Soc.* **1978**, *125*, 1328.

[67] A. Kudo, I. Mikami, *J. Chem. Soc., Faraday Trans.* **1998**, *94*, 2929.

[68] C. M. Leroy, A. E. Maegli, K. Sivula, T. Hisatomi, N. Xanthopoulos, E. H. Otal, S. Yoon, A. Weidenkaff, R. Sanjines, M. Gratzel, *Chem. Commun.* **2012**, *48*, 820.